Mechanical-Based Properties of Mine Tailings for Static Liquefaction

Luis Vergaray¹ and Jorge Macedo, Ph.D.²

¹Graduate Student, Dept. of Civil and Environmental Engineering, Georgia Institute of Technology, Atlanta. Email: luis.vergaray@gatech.edu

²Assistant Professor, Dept. of Civil and Environmental Engineering, Georgia Institute of Technology, Atlanta. Email: jorge.macedo@ce.gatech.edu

ABSTRACT

Static liquefaction has been associated with numerous recent failures of tailings storage facilities (TSFs) around the world. These failures lead to devastating consequences for the environment and civil infrastructure and lead to the loss of human lives. In this study, we present trends for the response of mine tailings to monotonic loading considering (1) triaxial tests, (2) bender element tests, and (3) consolidation tests performed on mine tailings. These materials have a broad range of states (i.e., from very loose to dense states), a range of particle size distributions (i.e., from silty sand to almost pure silt mine tailings), and a broad range of compressibility. The trends are evaluated in the context of static liquefaction using critical state soil mechanics concepts considering different state definitions. In particular, we present trends for shear strength (residual and peak), state and brittleness soil indexes, and excess pore pressure indexes. Finally, static liquefaction screening indexes are proposed based on the observed trends, highlighting that static liquefaction is just another facet of soil behavior under monotonic loadings, and hence it should be explained under a mechanistic framework.

INTRODUCTION

The static liquefaction of mine tailings has caused numerous recent failures, e.g., the 2014 Mount Polley disaster in Canada (Morgenstern et al., 2015), the 2015 Fundao failure in Brazil (Morgenstern et al., 2016), the 2018 Cadia failure in Australia (Morgenstern et al., 2019), and the 2019 Brumadinho failure in Brazil (Robertson et al., 2019). Such failures of tailings storage facilities (TSFs) have caused unprecedented devastating consequences for the environment, infrastructure damage as well as human losses. These failures have triggered international debates regarding the safety of TSF systems. In particular, the conditions that result in static liquefaction of mine tailings remain a considerable concern affecting the financial viability of mines and the willingness of governments to allow mining. In the U.S. exist approximately 1200 TSFs, with 60% of them having a significant hazard according to the USACE classification (USACE, 2016). Hence, the safety of TSFs is an important issue. As engineering practice is moving more towards finite element or finite difference-based stress analyses (e.g., the evaluations performed in the forensic studies after recent failures), understanding the mechanical response of mine tailings is also fundamental for the calibration of constitutive models that can later be used in numerical simulations. This is not simple because mine tailings are often characterized as intermediate materials (pure silts or sandy silts), which represents a fundamental challenge for understanding their mechanical response. Tailings are also geologically young materials, with angular grains rather than subrounded and often with lower proportions of quartz than many natural soils; thus, standard geotechnical correlations should not be taken as

applicable to tailings without detailed consideration of these factors. Previous efforts on understanding the trends in the mechanical response of particulate materials under monotonic loadings have been mainly focused on sands with low fine contents (e.g., Sadrekarimi, 2014; Jefferies and Been, 2016, Rabbi et al., 2019). In terms of mine tailings, the experimental studies that have evaluated their mechanical response and the associated mechanical parameters are somewhat limited compared to sand materials (e.g., Jefferies and Been, 2016; Shuttle and Jefferies, 2016; Fourie and Tshabalala, 2005; Carrera et al., 2011). In this study, we present trends for mechanical-based parameters that control the response of mine tailings, in the context of static liquefaction, which have not been previously explored considering a large set of tailings materials. The trends are presented using results from 53 mine tailings materials (including available data from the recent failures previously discussed), which have been processed in a uniform manner. Finally, we provide screening indexes to be used in engineering practice for the assessment of static liquefaction in mine tailings using insights from the observed trends.

DATABASE

The whole database consists has 53 different mine tailings material, 7 of them were generated as part of this study and the rest were compiled from Shuttle & Cunning (2007), Anderson & Eldridge (2011), Bedin et al. (2012), Schnaid et al. (2013), Been (2016), Li & Coop (2018), Li & Coop (2019), Raposo (2016), Torres (2016), Morgenstern et al. (2016), Riemer et al. (2017), Li (2017), Robertson et al. (2019), Macedo & Petalas (2019), Gill (2019), Reid & Fanni (2020), Reid et al. (2018), Reid et al. (2020), Fourie & Papageorgiou(2001), and Carrera (2011). The mine tailings database corresponds to different ores (i.e., gold, iron, silver, copper, zinc, platinum) covering a broad range of fine contents (FC = 0 - 100 %), initial confining stress $(20 - 6000 \, kPa)$, specific gravity (Gs = 2.63 - 4.89), and states (i.e., very loose to dense). The available laboratory tests for each material have been processed in a uniform manner. The following properties were evaluated for each material: (1) the critical state line (CSL), in the case of a linear CSL, the slope (λ_e) , and the altitude at 1kpa (Γ) are estimated using Eq. 1. In the case of a curve CSL, the parameters are a, b, and c, according to Eq. 2 are estimated; (2) the stress ratio at critical state (M_{tc}) , and the volumetric coupling (N), according to Eq. 3; (3) the state-dilatancy parameter (χ), according to Eq. 4; and 4) the stiffnessconfinement dependence parameters (A, B) according to Equations 5 to 7. M_{tc} was estimated as the slope of the line that joins the ultimate points in a p (mean stress) versus q (deviatoric) plots or using Eq. 3, which is based on the strength-dilatancy relationship used in Jefferies and Been (2016). In Eq. 3, D_{min} represents the maximum dilatancy, and η_{max} is the maximum stress ratio. D_{min} was selected by plotting D versus the state parameter (ψ) , after getting rid of potential fluctuations (noise) using a loess non-parametric fitting. η_{max} was selected from a η versus axial strain plot. N was also calculated from Eq. 3., using the slope of the η_{max} versus D_{min} relationship. χ was calculated from a plot of D_{min} versus ψ , according to Eq. 4. Finally, the parameters A and B were calculated by non-linear regressions of the shear modulus (G) measured in the bender element tests versus the mean effective stress p according to Equations 5 to 7, using the two different functional forms. Equation 6 and 7 represent the functional form proposed by Hardin and Richart (1963) and Pestana and Whittle (1995), respectively.

$$e_c = \Gamma - \lambda_e \ln p \tag{1}$$

$$e_c = a - b \left(\frac{p}{p_{atm}}\right)^c \tag{2}$$

$$\eta_{max} = M_{tc} + (1 - D_{min})N \tag{3}$$

$$D_{min} = \chi \psi \tag{4}$$

$$G = A. F(e). \left(\frac{p}{p_a}\right)^B \tag{5}$$

$$F(e) = \frac{(2.97 - e)^2}{(1 + e)} \tag{6}$$

$$F(e) = \frac{1+e}{e} \tag{7}$$

An example of the calculation of these parameters I shown in Figure 1. Fig. 1a shows the estimation of the CSL, Fig. 1b shows the η_{max} versus D_{min} plot to estimate M_{tc} and N, Fig. 1c shows the state-dilatancy relationship to estimate χ , and Fig. 1d shows the G versus p plot to estimate A and B, according to equation 3a.

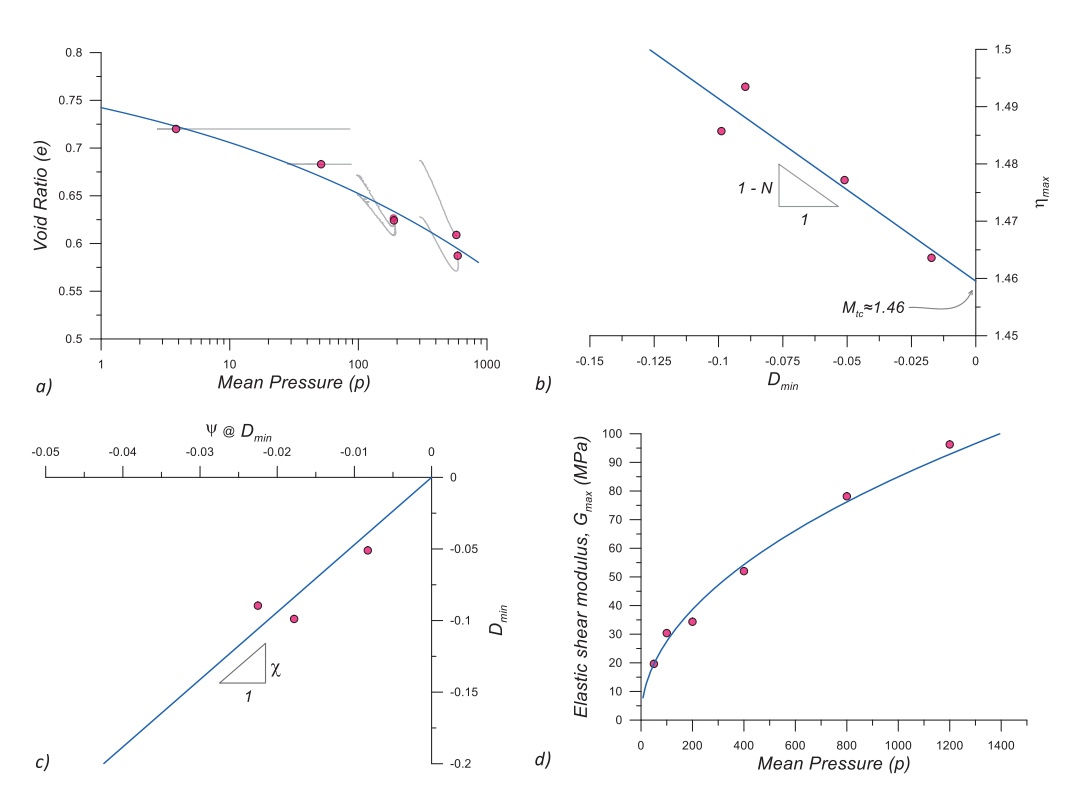


Figure 1. Illustration of the estimation of a) CSL estimation, b) η_{max} versus D_{min} plot to estimate M_{tc} and N, c) state-dilatancy relationship to estimate χ , and d) G versus p plot to estimate A, and B.

It is important to highlight that Γ , λ_e , M_{tc} , N, χ , A, and B are often present as parameters in robust constitutive models, usually formulated for sands (although often named differently or represented by other proxies) and are the basis for the current mechanical-based understanding of static liquefaction. In the case of undrained triaxial tests, we classified each test as a) flow liquefaction with full softening, b) flow liquefaction with partial softening, c) limited flow liquefaction, and d) non-flow liquefaction. This classification is consistent with that in Rabbi et al. (2019). The subdivision of flow liquefaction cases in full softening and partial softening is also consistent with Soares and Viana da Fonseca (2016).

TRENDS IN THE MECHANICAL RESPONSE OF MINE TAILINGS

Stiffness: Due to the the angularity associated with mine tailings as a product of the mineral processing, the M_{tc} values for mine tailings are generally larger compared to sands as shown in Figure 2a, which has also been observed in previous studies (e.g., Reid, 2015). Figure 2b, shows the variation of the A coefficient with the initial state parameter, suggesting a good correlation. Hence, larger A values are generally associated with dense materials and lower A values are generally associated with loose materials. Furthermore, parameters A and B have shown to be dependent on particle shape and grain size distribution in sands (Cho et al., 2006; Payan et al., 2015). A, specifically, represents a volumetric-blended measure of soil particle stiffness. We explored the stiffness dependence on the particle size distribution of mine tailings using the α and β parameters ($V_s = \alpha (p/1kpa)^{\beta}$, where V_s is the shear wave velocity from bender tests). α and β are shear wave velocity counterparts of A and B and are used to integrate the sand data from Cho et al. (2006) in Fig. 2c and 2b.

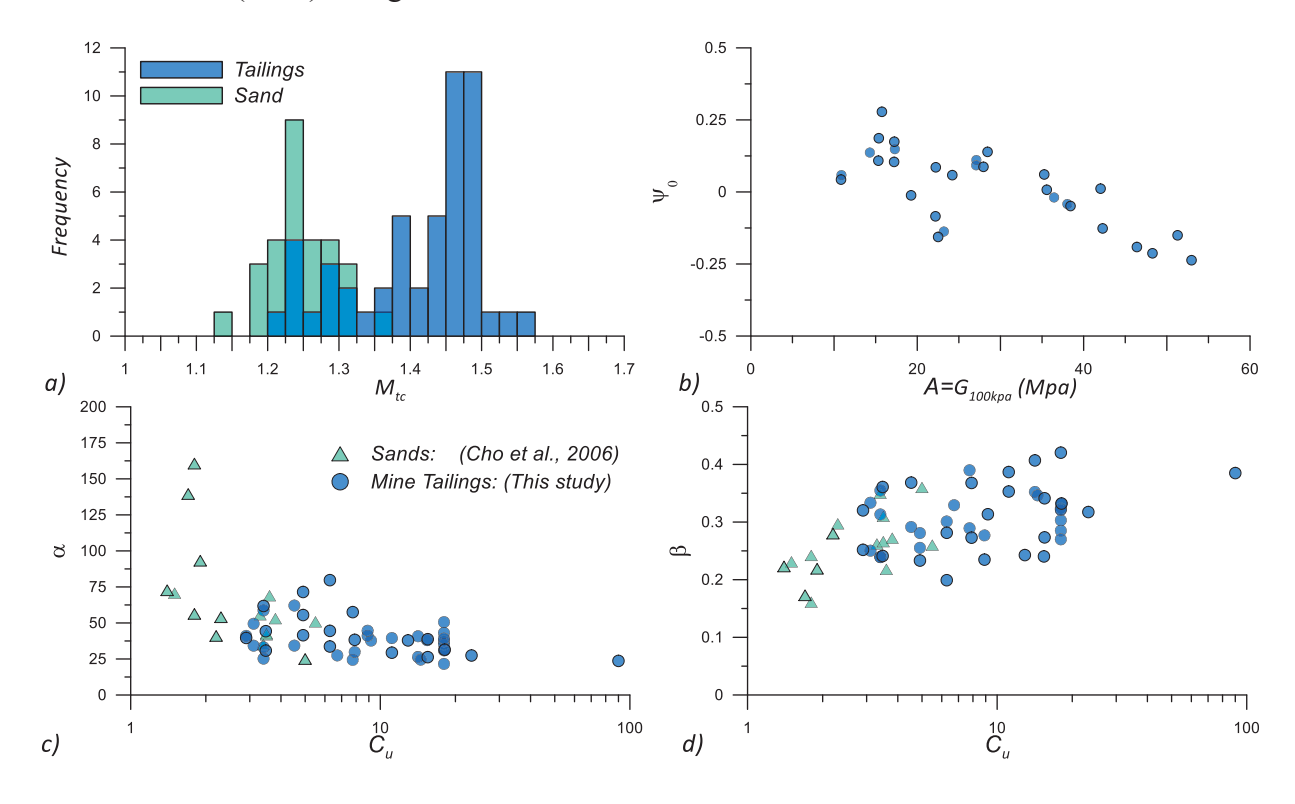


Figure 2. a) Distribution of M_{tc} values for tailing and sands, b) A versus ψ_0 , c) Variation of α and C_u and d) Variation of β and C_u .

The trends indicate that as C_u increases α decreases and β increases. This is consistent with Payan et al. (2015) and suggest that the overall effect of the irregularities introduced by different particle sizes is to hinder particle mobility and their ability to attain dense packing configurations leading to lower V_s (lower α) that are more susceptible to changes in stresses (higher β).

Residual and peak strength: The peak and residual shear strengths (Su_r/σ'_0) and Su_r/σ'_0 , respectively) are presented in Figure 3 in terms of the brittleness index (I_b) and ψ_0 . Fig. 3a, and Fig. 3b shows the variations of Su_r/σ'_0 and I_b , along with upper and lower bound trends for sand materials extracted from Sadrekarimi (2014). It is noticed that, in general, the trends are reasonably consistent. Fig. 3c shows the variation of Su_r/σ'_0 in terms of ψ_0 along with similar trends for sands with different compressibility (including the Lagunillas sandy silt) extracted from Sadrekarimi (2013). Fig. 3d shows the variation of Su_y/σ'_0 in terms of and ψ along with upper and lower bound trends for Su_y/σ'_0 in sands extracted from Jefferies and Been (2016). By examining Fig. 3c, the effect of compressibility is clearly observed, i.e., Su_r/σ'_0 in the case of sand materials increases with the increase of compressibility. In particular, the trends extracted for the Lagunillas sandy silt are more consistent with the overall variation of strength for mine tailings.

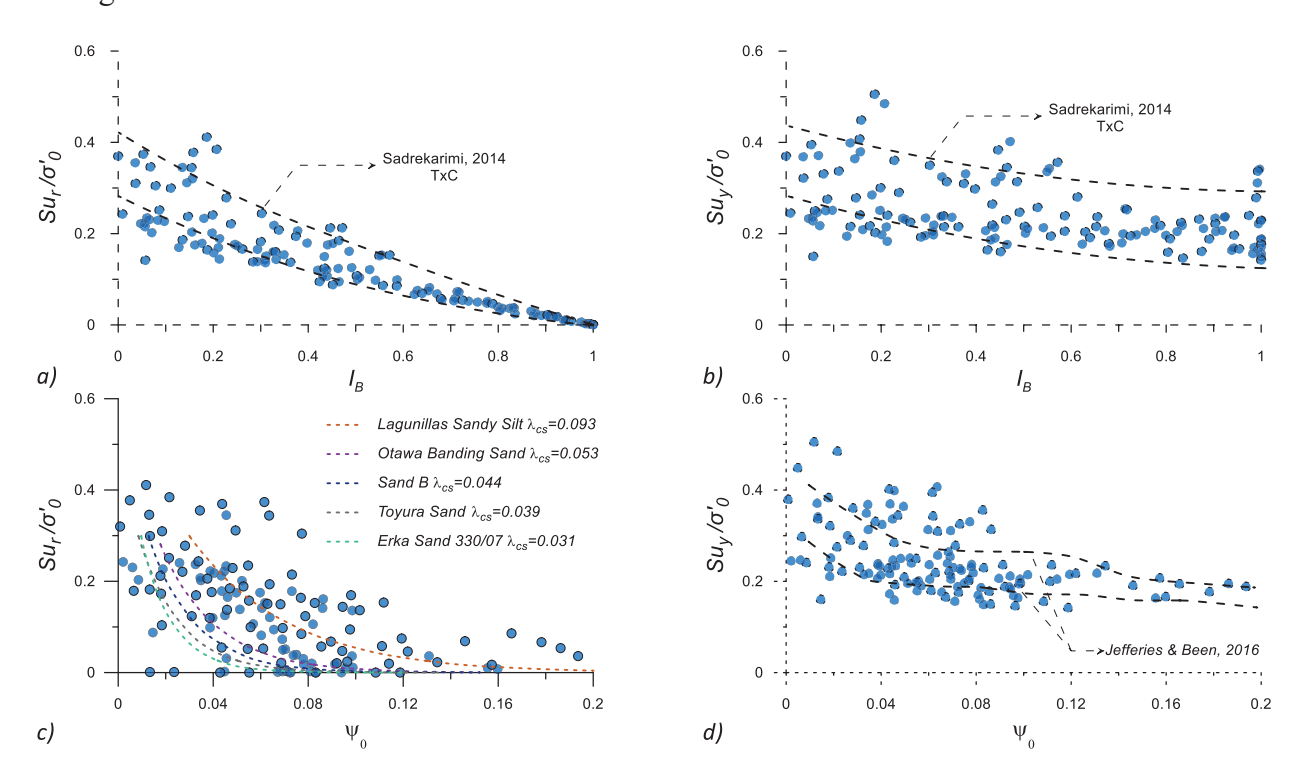


Figure 3. Variation of Su_r/σ'_0 and Su_y/σ'_0 vs the brittleness index ((a) and (b), respectively); and Su_r/σ'_0 and Su_y/σ'_0 vs the initial state parameter (ψ_0) ((c) and (d), respectively).

The variation of Su_y/σ'_0 in Fig. 3d suggests that Su_y/σ'_0 tends to be larger in mine tailings compare to the sands in Jefferies and Been (2016) when ψ is lower than 0.1. To bring the effects of compressibility, we normalized the state parameter by λ_e . A similar effect can be observed in terms of Su_y/σ'_0 in Fig. 4b, which shows that the normalization of ψ also helps to decrease the

scatter. To account for the effects of angularity in strength, we further normalized the Su_r/σ'_0 and Su_y/σ'_0 ratios by M_{tc} , and plotted the results in terms of ψ/λ_e . The results are shown in Figure 4 c and d. Recall that from CSSM concepts (e.g., Jefferies and Been, 2016) $Su_r/(M\sigma'_0) = 0.5exp(-\psi/\lambda_e)$, which is also plotted in Figure 4c. This normalization brings an additional (minor) reduction to the scatter in the trends because compressibility and angularity effects are now considered through λ_e and M_{tc} .

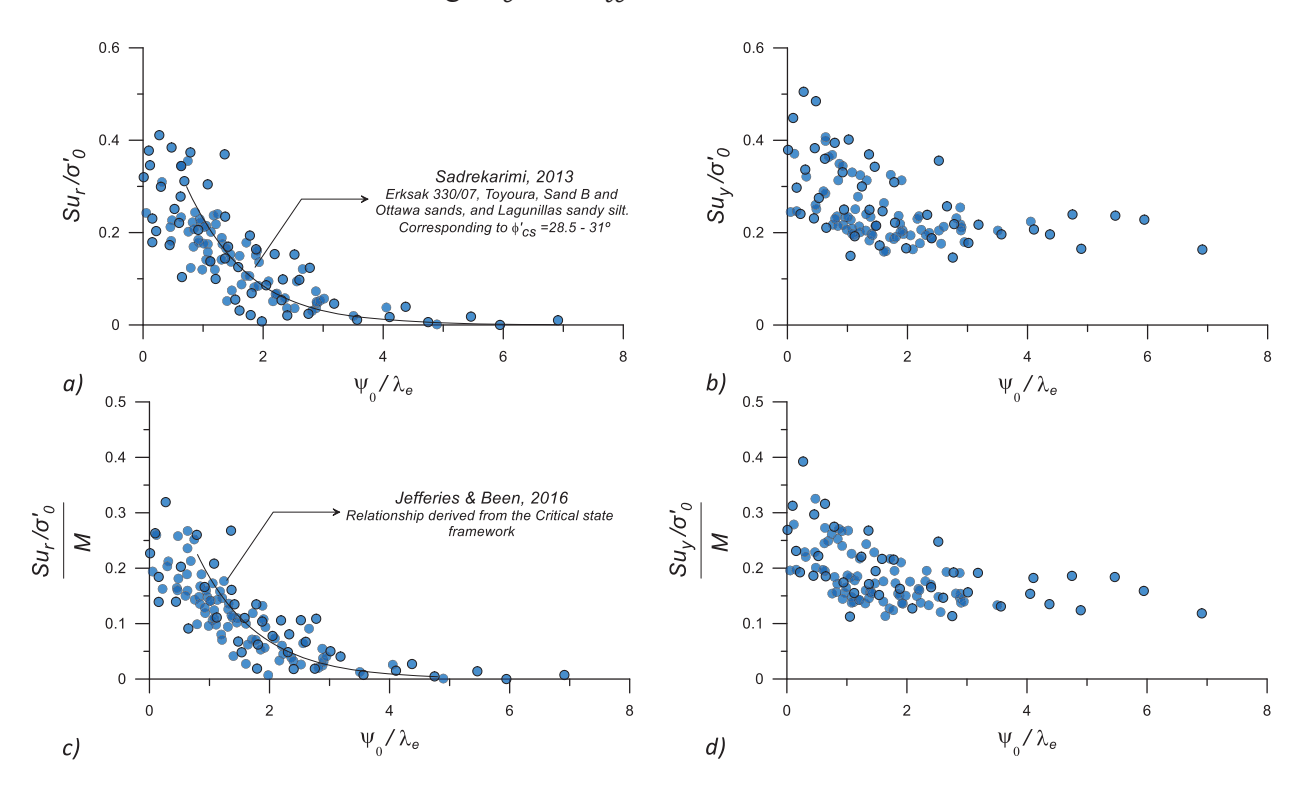


Figure 4. Variation of Su_r/σ'_0 and Su_y/σ'_0 versus ψ_0/λ_e ((a) and (b), respectively); and $Su_r/(M_{tc}\sigma'_0)$ and $Su_y/(M\sigma'_0)$ versus ψ_0/λ_e ((c) and (d), respectively).

State and brittleness and instability stress ratio: The flow liquefaction cases that correspond to full softening and partial softening, are presented in Figure 5 as red and yellow points, respectively. Figure 5a and 5b shows the relationship between parameters to represent the state and brittleness of a soil material. Fig. 5a shows the relationship between I_b and ψ/λ_e , along with the data from Smith et al. (2019), and the upper and lower bounds they proposed. It can be observed that our data is consistent with these upper and lower bounds. Of note, the trends suggest that flow liquefaction cases with partial softening may have in general a I_b larger than 0.25 and a ψ/λ_e larger than 0.75, whereas the flow liquefaction cases with full softening may be associated with I_b values higher than 0.6 and ψ/λ_e values larger than 1.5. Fig. 4b shows the relationship between I_b and the pressure index $I_p = p_0/p_{crit}$ (where p_0 and p_{crit} are the effective mean pressure at the initial and critical state, respectively). As expected I_p increases with the increase of I_b , and I_p values higher than 2.5 seem to be indicative of flow liquefaction with partial softening, whereas values larger than 10 may be indicative of potential flow liquefaction with full softening. Figure 5c shows the variation of the normalized instability stress ratio η_{IL}/M_{tc} and the normalized state parameter (ψ_0/λ_e) , for the cases where partial or full

softening (i.e., flow liquefaction) was observed in undrained triaxial tests. As expected, η_{IL}/M_{tc} tends to decrease with the increase of increase of ψ_0/λ_e . In addition, we observe η_{IL}/M_{tc} values that are generally in the range of 0.6 to 1 for flow liquefaction cases with partial softening, and values lower than 0.6 for flow liquefaction cases with full softening.

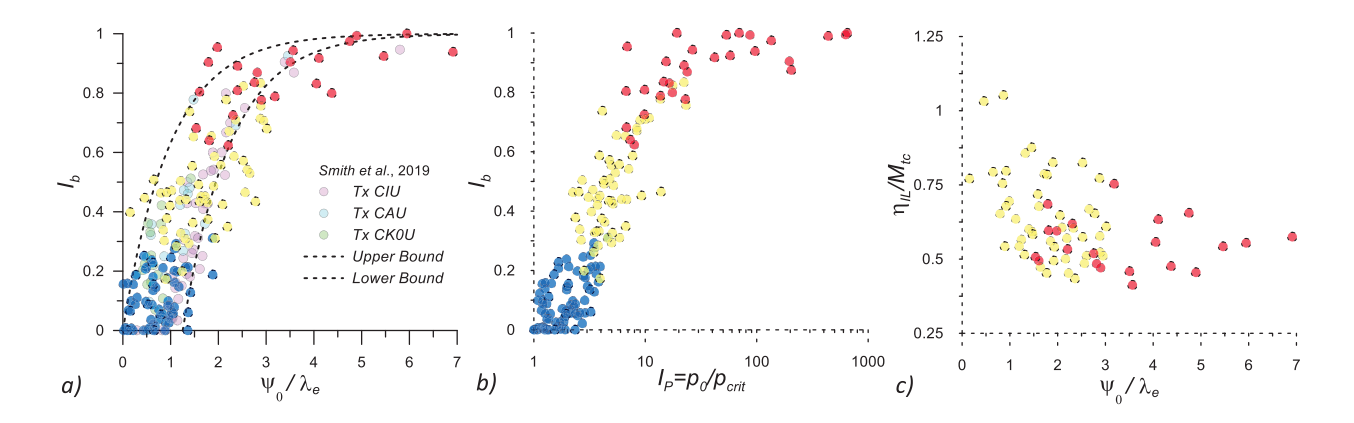


Figure 5. a) Relationship between I_b and ψ/λ_e , b) I_b versus I_p and c) Variation of the normalized instability stress ratio $({\eta_{IL}}/{M_{tc}})$ versus ψ/λ_e .

Excess pore pressures: The variation of $r_u = \Delta u/\sigma'_0$ versus I_b along with the trend of r_u relationships for sands considering triaxial extension (TxE), plane strain compression (PSC), and triaxial compression (TxC) conditions are presented on Figure 6. The TxE and PSC trends were extracted from Sadrekarimi (2016), and the TxC trends were extracted from Sadrekarimi (2020). In general, it can be observed that flow liquefaction cases (partial and full softening) show r_u values large than 0.8, and the data is generally consistent with the average trend extracted for sand materials, but it is observed that the r_u values in mine tailings tend to be larger compared to sands in cases with partial softening. Fig. 6b shows the r_u variation in terms of ψ . In general, large r_u values were observed with most values higher than 0.6 for $\psi > 0$. As expected r_u increases with the increase in I_b and ψ ; and an I_b higher than 0.1 or a ψ higher than 0 are indicative or large excess pore pressure generation (i.e., $r_u > 0.6$).

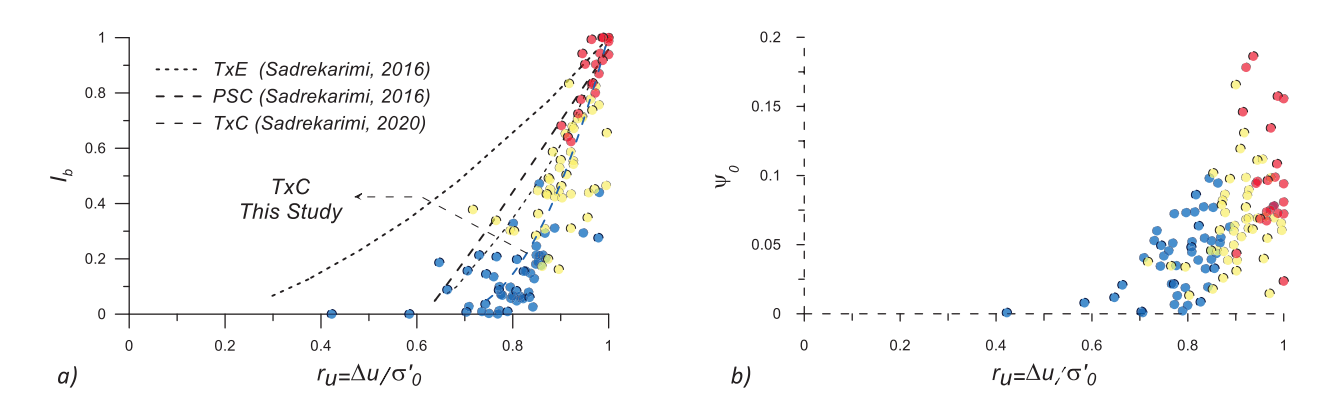


Figure 6. Variation of r_u vs a) the brittleness index, and b) state parameter.

CONCLUSIONS

In this study, we have used critical state soil mechanics (CSSM) concepts to examined salient trends on the mechanical response of mine tailings in the context of static liquefaction, highlighting the role the relative proportions of different particles sizes, and particle properties. Our results suggest that mine tailings fit the same framework as natural sands, with the key difference of showing a much larger M_{tc} . Thus, the mechanical response of mine tailings can be reasonably well explained once CSSM-based parameters such as Γ , λ_e , ψ , M_{tc} , χ , N, and G are incorporated. Additional salient conclusions from this study include:

- The M_{tc} values in mine tailings (in the order of 1.4) are larger, on average, compared to M_{tc} values on natural sands (in the order of 1.2). This is associated to the particle shape of mine tailings, which tend to have more angular particles compared to the subrounded grains found in natural soils.
- Using the functional forms from Hardin and Richart (1963) and Pestana and Whittle (1995) for G (Equation 3), we observed that the parameter A that controls the magnitude of G correlates well with ψ_0 . In addition, the parameter B that controls the dependence on p, generally varies from 0.4 to 0.8.
- Compressibility can have an important effect on Su_r/σ'_0 , and also controls Su_y/σ'_0 . Hence, it should be carefully considered in evaluating appropriate Su_r/σ'_0 and Su_y/σ'_0 design values.
- The trends suggest that flow liquefaction cases with partial softening may have in general I_b, ψ/λ, and I_p values larger than 0.25, 0.75, and 2.5, respectively. Whereas flow liquefaction with full softening is associated with I_b, ψ/λ, and I_p values higher than 0.6, 1.5, and 10, respectively. We recommend using these values as part of screening procedures in engineering practice.

ACKNOWLEDGMENTS

This study has been funded by the National Science Foundation (NSF) under the CMMI 2013947 project and has also received support from the TAilings and IndustriaL waste ENGineering Center (TAILENG). We also thank Mr. Terry Eldridge, Mr. Mike Jefferies, and Dr. Li Wei, who kindly share data on mine tailings and sand materials.

REFERENCES

- Anderson, C., and Eldridge, T. (2011). Critical state liquefaction assessment of an upstream constructed tailings sand dam. *Tailings and Mine Waste 2010*.
- Bedin, J., Schnaid, F., Da Fonseca, A. V., and Costa Filho, L. D. M. (2012). Gold tailings liquefaction under critical state soil mechanics. *Géotechnique*, 62(3):263–267.
- Been, K. (2016). Characterizing mine tailings for geotechnical design. *Geotechnical and Geophysical Site Characterisation 5*. Australian Geomechanics Society, Sydney, Australia, 41–56.
- Carrera, A., Coop, M., and Lancellotta, R. (2011). Influence of grading on the mechanical behaviour of Stava tailings. *Géotechnique*, 61(11):935–946.

- Cho, G.-C., Dodds, J., and Santamarina, J. C. 2006. "Particle Shape Effects on Packing Density, Stiffness, and Strength: Natural and Crushed Sands." *Journal of Geotechnical and Geoenvironmental Engineering*, 132(5):591–602.
- Fourie, A. B., and Papageorgiou, G. (2001). Defining an appropriate steady state line for Merriespruit gold tailings. *Canadian Geotechnical Journal*, 38(4):695–706.
- Fourie, A. B., and Tshabalala, L. (2005). Initiation of static liquefaction and the role of K0 consolidation. *Canadian Geotechnical Journal*, 42(3):892–906.
- Gill, S. S. (2019). *Geotechnical properties of tailings: effect of fines content*. University of Toronto.
- Hardin, B. O., and Richart, F. E. (1963). Elastic wave velocities in granular soils. *Journal of the Soil Mechanics and Foundations Division*, ASCE, 89(SM1):33-65.
- Jefferies, M. G., and Been, K. (2016). *Soil liquefaction: a critical state approach*. 2nd edn. Boca Raton, FL, USA: CRC Press.
- Li, W. (2017). *The mechanical behaviour of tailings*. PhD. Thesis, City University of Hong Kong, Hong Kong.
- Li, W., and Coop, M. R. (2019). Mechanical behaviour of Panzhihua iron tailings. *Canadian Geotechnical Journal*, 56(3):420–435.
- Li, W., Coop, M. R., Senetakis, K., and Schnaid, F. (2018). The mechanics of a silt-sized gold tailing. *Engineering Geology*, 241, 97–108.
- Macedo, J., and Petalas, A. (2019). Calibration of Two Plasticity Models against the Static and Cyclic Response of Tailings Materials. *Proceedings of Tailings and Mine Waste 2019*, Vancouver.
- Morgenstern, N. R., Jefferies, M., Zyl, D., and Wates, J. (2019). Independent Technical Review Board. Report on NTSF Embankment Failure. Ashurst Australia.
- Morgenstern, N. R., Vick, S. G., Viotti, C. B., and Watts, B. D. (2016). Fundao tailings dam review panel. Report in the immediate causes of the failure of the Fundao Dam. New York: Cleary Gottlieb Steen and Hamilton LLP.
- Morgenstern, N. R., Vick, S. G., and Zyl, D. (2015). Independent Expert Engineering Investigation and Review Panel." Report on Mount Polley Tailings Storage Facility Breach. British Columbia.
- Payan, M., Khoshghalb, A., Senetakis, K., and Khalili, N. 2015. "Effect of particle shape and validity of Gmax models for sand: A critical review and a new expression." *Computers and Geotechnics*, 72:28–41.
- Pestana, J. M., and Whittle, A. J. (1995). Compression model for cohesionless soils. *Géotechnique*, 45(4):611–631.
- Rabbi, A. T. M. Z., Rahman, M. M., and Cameron, D. A. (2019). The relation between the state indices and the characteristic features of undrained behaviour of silty sand. *Soils and Foundations*, 59(4):801–813.
- Raposo, N. (2016). Deposição de rejeitados espessados. caraterização experimental e modelação numérica. PhD. Thesis, University of Porto.
- Reid, D. (2015). Estimating slope of critical state line from cone penetration test an update. *Canadian Geotechnical Journal*, 52(1), 46–57.
- Reid, D., and Fanni, R. (2020). A comparison of intact and reconstituted samples of a silt tailings. *Géotechnique*, 1–13. Available at:.
- Reid, D., Fanni, R., Koh, K., and Orea, I. (2018). Characterisation of a subaqueously deposited silt iron ore tailings. *Géotechnique Letters*, 8(4):278–283.

- Reid, D., Fourie, A., Ayala, J. L., Dickinson, S., Ochoa-Cornejo, F., Fanni, R., Garfias, A., Da Fonseca, A., Ghafghaz, M., Ovalle, C., Riemer, M., Rismanchian, A., and Suazo, G. (2020). Results of a critical state line testing round robin programme. *Géotechnique*, 1-15.
- Riemer, M., Macedo, J., Roman, O., and Paihua, S. (2017). Effects of stress state on the cyclic response of mine tailings and its impact on expanding a tailings impoundment. *3rd International Conference on Performance-based Design in Earthquake Geotechnical Engineering*. Vancouver.
- Robertson, P. K., De Melo, L., Williams, D. J., and Wilson, G. W. (2019). Report of the Expert Panel on the Technical Causes of the Failure of Feijão Dam I.
- Sadrekarimi, A. (2013). Influence of state and compressibility on liquefied strength of sands. *Canadian Geotechnical Journal*, 50(10):1067–1076.
- Sadrekarimi, A. (2014). Effect of the mode of shear on static liquefaction analysis. *Journal of Geotechnical and Geoenvironmental Engineering*, 140(12):04014069.
- Sadrekarimi, A. (2016). Static Liquefaction Analysis considering principal stress directions and anisotropy. *Geotechnical and Geological Engineering*, 34(4):1135–1154.
- Sadrekarimi, A. (2020). Forewarning of Static Liquefaction Landslides. *Journal of Geotechnical and Geoenvironmental Engineering*, 146(9), 04020090.
- Schnaid, F., Bedin, J., Viana da Fonseca, A. J. P., and Costa Filho, L. D. (2013). Stiffness and strength governing the static liquefaction of tailings. *Journal of Geotechnical and Geoenvironmental Engineering*, 139(12):2136–2144.
- Shuttle, D. A., and Cunning, J. (2007). Liquefaction potential of silts from CPTu. *Canadian Geotechnical Journal*, 44(1):1–19. Available at:.
- Shuttle, D., and Jefferies, M. (2016). Determining silt state from CPTu. *Geotechnical Research*, 3(3):90–118.
- Smith, K., Fanni, R., Capman, P., and Reid, D. (2019). Critical State Testing of Tailings: Comparison between Various Tailings and Implications for Design. *Proceedings of Tailings and Mine Waste 2019*. Vancouver.
- Soares, M., and da Fonseca, A. V. (2016). Factors affecting steady state locus in triaxial tests. *Geotechnical Testing Journal*, 39(6): 1056-1078.
- Torres, L. A. (2016). *Use of the cone penetration test to assess the liquefaction potential of tailings storage facilities*. PhD. Thesis, University of the Witwatersrand, Johannesburg. USACE. (2016). *National inventory of dams*. Army Corp of Engineers.